Tunable Arrangement of Gold Nanoparticles in Epoxidated Poly(styrene-*block*-butadiene) Diblock Copolymer Matrices

Shiao-Wei Kuo,* Hong-Ying Yang

A new approach to synthesize block-copolymer-mediated/gold nanoparticle (Au NP) composites is developed. Stable and narrowly distributed Au NPs modified with a 2-phenylethanethiol ligand are prepared by a two-phase liquid–liquid method. A new epoxidation of a poly(styrene-*block*-butadiene) diblock copolymer, to form poly(styrene-*block*-vinyl oxirane) (PS-*b*-PBO), is achieved through chemical modification. It is found that the Au NPs disperse well in the PS block segment by partially crosslinking the PBO block segment with poly(ethylene oxide bisamine) (D230), a curing agent. The aggregation of Au NPs leads to a red-shift of the plasmon absorption with the increase in the D230 content. However, without crosslinking the PBO block segment with D230, Au NPs distributes in both the PS and PBO segments.

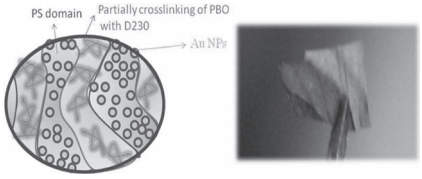

1. Introduction

Metal and semiconductor nanoparticles (NPs) possess unique electronic and chemical properties because of their large surface areas and confinement of electronic states.[1,2] Gold nanoparticles (Au NPs)[3–5] have recently been used in many applications in industrial chemistry, such as in low-temperature CO oxidation,[6] hydrocarbon hydrogenation,[7,8] low-temperature hydrocarbon oxidation,[9,10] and NO reduction.[11] Au NPs enclosed within self-assembled block copolymer templates provide new opportunities for the development of functional hybrid materials exhibiting enhanced optical, electrical, and mechanical properties.[12–14] For instance, diblock copolymers can form a variety of self-assembled structures with periodic features on nanometer length scales ranging between 10 and 100 nm.[15,16] Because NPs are between 1 and 10 nm in size, using diblock copolymers as templates to control the positions of NPs spatially is a natural approach toward the production of hierarchically ordered structures.[17–20] In addition, block copolymer/NP composites are fascinating model systems for studying the mechanisms of structure formation in soft/hard heterogeneous materials.[21–24]

The incorporation of Au NPs into diblock polymer matrices through NP–polymer matrix interactions is an important subject in materials engineering; therefore, various attempts have been made to create block-copolymer-mediated nanocomposites.[25–32] In general, the protonated pyridyl nitrogen atoms of poly(4-vinyl pyridine) blocks form ionic bonds with $AuCl_4^-$ ions and coordinate with the Au NPs formed after the reduction of these ions.[33–35] As a result, poly(styrene-*block*-vinyl pyridine) (PS-*b*-PVP)[19,36–38] or poly(ε-caprolactone-*block*-4-vinyl pyridine) (PCL-*b*-P4VP)[39,40] can be prepared to capture $AuCl_4^-$ ions from water and to recycle Au NPs into organic solvents. In addition, diblock copolymers with site-selective Au NPs may prohibit the possible formation of macroscopic aggregates, leading to mixtures of NPs homogeneously dispersed throughout a composite film.

In a study by Corbierre, alkanethiol-decorated Au NPs proved difficult to disperse in non-polar polymers such as polystyrene (PS) and poly(dimethyl siloxane) (PDMS).[41]

Dr. S. W. Kuo, Dr. H.-Y. Yang
Department of Materials and Optoelectronic Science, Center for Nanoscience and Nanotechnology, National Sun Yat-Sen University, Kaohsiung, Taiwan, Republic of China
E-mail: kuosw@faculty.nsysu.edu.tw

DOI: 10.1002/macp.201100360

Au NP aggregates, several hundreds of nanometers in dimension, were always formed in the PS matrices. One approach to overcome these difficulties involves the incorporation of a polymer ligand (such as thiol-capped polystyrene, PS-SH), the chemical structure of which is similar to that of a PS matrix, to make the NPs more thermodynamically favorable for incorporation.[38,41–43] The incorporation of low-molecular-weight surfactant-stabilized Au NPs in a PS matrix remains a challenge.[41] Wei et al. reported the packing of 2-phenylethanethiol Au NP clusters in the PS domain of a PS-*b*-P4VP block copolymer, which, after thermal annealing at high temperature (170 °C), formed a NP-filled shell-like assembly as a result of the evaporation of the 2-phenylethanethiol ligands. The partial loss of the hydrophobic thiol ligands from the Au NP surfaces was compensated by the surrounding pyridine groups of the P4VP domains when the Au NPs diffused to the PS/P4VP interface.[44]

In this paper, we report the fabrication of an epoxidated poly(styrene-*block*-butadiene) (PS-*b*-PB) copolymer film, poly(styrene-*block*-vinyl oxirane) (PS-*b*-PBO), that enables position control of 2-phenylethanethiol-coated Au NPs, which selectively locate in the PS rather than the PBO domain after solvent evaporation because of the greater affinity afforded by the π–π interactions between the phenyl groups of the Au NPs and PS segments. However, π–π interactions are significantly weaker than ionic interactions between Au NPs and P4VP; in fact, 2-phenylethanethiol Au NPs are difficult to disperse in a PS matrix and exhibit strong aggregation in the PS-*b*-PBO block copolymer into structures several hundreds of nanometers in dimension. As a result, the partial crosslinking of PS-*b*-PBO with poly(ethylene oxide bisamine) (D230), a curing agent, is necessary to prohibit Au NP aggregation and diffusion into PBO domains. In our study, the controlled interparticle distance of the Au NPs in the diblock copolymer film gives rise to a broad tunability of the coupled plasmon frequency ranging from 500 to 550 nm of the two NPs as a function of the degree of crosslinking of PS-*b*-PBO with the D230 curing agent. We used small-angle X-ray scattering (SAXS) and transmission electron microscopy (TEM) to observe the self-assembled morphology of the block copolymer and the diffusion of hydrophobic Au NPs from hydrophobic PS domains to hydrophilic PBO domains.

2. Experimental Section

2.1. Materials

The diblock polymer used in this study, PS-*b*-PB (1,2 addition) with a polydispersity index $\overline{M}_w/\overline{M}_n = 1.09$, was synthesized by sequential anionic polymerization of styrene and butadiene (Polymer Source, Inc.). The degree of polymerization of styrene and butadiene was 1906 and 1796, respectively. Poly(ethylene oxide bisamine) with a molecular weight of 230 g mol^{-1} (Jeffamine, D230) and *meta*-chloroperoxybenzoic acid were purchased from Aldrich Co. Dichloromethane, chloroauric acid ($HAuCl_4$), 2-phenylethanethiol, tetraoctylammonium bromide (TOAB), sodium borohydride ($NaBH_4$), and toluene were purchased from Acros Organics.

2.2. The Epoxidation of PS-*b*-PB

PS-*b*-PB diblock copolymer was dissolved at ambient temperature in dichloromethane (≈0.7 M) and then cooled to 0 °C. The solution was stirred for 10 min, and then 0.1 M *meta*-chloroperoxybenzoic acid was added. After stirring the solution for 72 h at 0 °C, the epoxidated product PS-*b*-PBO was obtained through precipitation in methanol and dried under high vacuum. The synthesis is summarized in Scheme 1.

2.3. The Synthesis of 2-Phenylethanethiol Au NPs

The 2-phenylethanethiol Au NPs used in this study were prepared using standard Brust–Schiffrin methodology.[45] A typical synthesis proceeded as follows: 30 mL of an aqueous solution of $HAuCl_4$ (0.24 mmol) was stirred with a solution of TOAB (0.34 g) in 80 mL of toluene until all of the $HAuCl_4$ was transferred to the organic layer. A total of 0.68 μL of 2-phenylethanethiol was then added to the organic phase. After stirring for 2 h, 50.0 mL of a freshly prepared 0.40 M $NaBH_4$ solution was added over 20 min, and the solution was stirred for the next 24 h. Excess thiol, free disulfide, and TOAB impurities were removed during size-selective precipitations of the Au NPs with acetone/ethanol/methanol mixtures. Larger Au NPs were formed by refluxing the smaller Au NPs in toluene in the presence of TOAB (half the molar amount of Au) for different time intervals, followed by a similar size-selective precipitation and purification as described previously.

2.4. The Preparation of PS-*b*-PBO/Au NP Composites without Crosslinking

Mixtures of PS-*b*-PBO with different Au NP contents were prepared through solution blending. Toluene solutions containing 20 wt% of the PS-*b*-PBO diblock copolymers were stirred for 6–8 h, the solvent was then left to evaporate slowly at room temperature for 24 h. The PS-*b*-PBO/Au NP films were then dried at 50 °C for 2 d.

2.5. The Preparation of PS-*b*-PBO/Au NP Composites with Partial Crosslinking using Poly(ethylene oxide bisamine)

Stoichiometric amounts of poly(ethylene oxide bisamine) (D230) with PS-*b*-PBO diblock copolymer (20 wt% in solution) were mixed in a high-speed stirrer in a toluene solution, solution cast, and then dried under vacuum. The cast film was crosslinked at 90 °C for 20 min, and 3 wt% of Au NPs in toluene was then added to the partially crosslinked PS-*b*-PBO cast films and stirred for 24 h. The films containing partially crosslinked PS-*b*-PBO with Au NPs were then dried at 50 °C for 2 d.

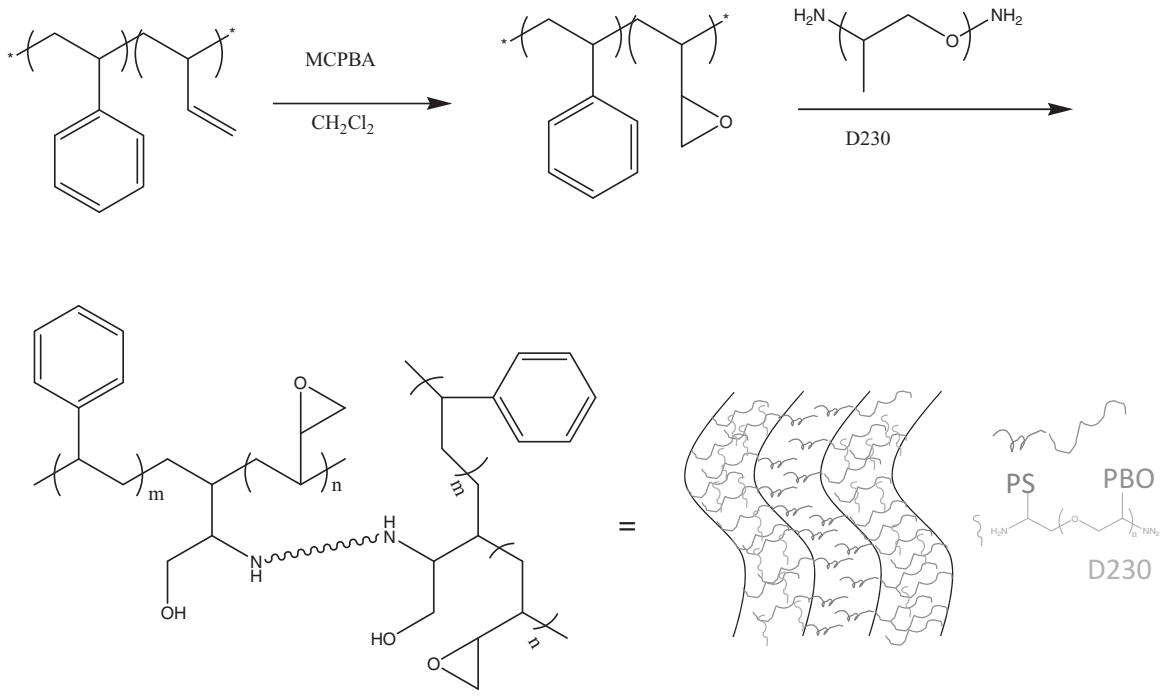

Scheme 1. The synthesis of PS-*b*-PBO and the crosslinking reaction with poly(ethylene oxide bisamine) curing agent.

2.6. Characterization

^{1}H NMR spectra were recorded at room temperature using a Bruker AM 500 (500 MHz) spectrometer, with the residual proton resonance of the deuterated solvent as the internal standard. Fourier transform infrared (FT-IR) spectra of the polymer blend films were recorded using the conventional KBr disk method. The film used in this study was sufficiently thin enough to obey the Beer–Lambert law. FT-IR spectra were recorded using a Bruker Tensor 27 FT-IR spectrophotometer; 32 scans were collected at a spectral resolution of 1 cm^{-1}. IR spectra of the samples were recorded at elevated temperatures using a cell mounted within the temperature-controlled compartment of the spectrometer. The glass transition temperatures (T_g) of the diblock copolymer films were determined through DSC using a TA Q-20 instrument. The scan rate was 20 °C min^{-1} within the temperature range 30–120 °C; the temperature was then held at 120 °C for 3 min to ensure the complete removal of residual solvent. T_g measurements were performed in the DSC sample cell after the sample (5–10 mg) had been cooled rapidly to –90 °C from the melt of the first scan. The T_g was defined as the midpoint of the heat capacity transition between the upper and lower points of deviation from the extrapolated liquid and glass lines. TGA was performed under nitrogen or air using a TA Q50 thermogravimetric analyzer at a heating rate of 20 °C min^{-1} from room temperature to 800 °C. The rate of nitrogen or air flow was 60 mL min^{-1}. UV-vis spectra (DU700, Beckmann) were used to characterize the aggregation of Au NPs from 400–750 nm. The size distributions of the gold core in the aggregates were measured by TEM (JEOL JEM-1200CX). Ultrathin sections of the samples were prepared using a Leica Ultracut S microtome equipped with a diamond knife. Slices of ≈700 Å in thickness were cut at room temperature. The ultrathin sections were placed onto copper grids coated with carbon-supporting films and then stained by exposure to the vapor of a 4% RuO_4 aqueous solution for 30 min. Because RuO_4 is a preferential staining agent, it made the PS domains appear dark and the PBO domains appear bright in the micrographs, respectively. SAXS measurements were taken on a Nanostar U small-angle X-ray scattering system (Bruker, Germany) using Cu Kα radiation (40 kV, 35 mA). The *d*-spacing values were calculated using the formula $d = 2\pi/q$.

3. Results and Discussion

3.1. The Synthesis of the PS-*b*-PBO Copolymer

Figure 1 shows the ^{1}H NMR spectra of the PS-*b*-PB and PS-*b*-PBO diblock copolymers; the signals attributable to the aromatic protons were observed at 6.5–7.1 ppm from the PS block. These signals did not change after epoxidation with *meta*-chloroperoxybenzoic acid. However, the double bond ($HC=CH_2$) from polybutadiene was located at 4.9, 5.1, and 5.3 ppm; these signals almost disappear after epoxidation with *meta*-chloroperoxybenzoic acid. New signals were observed at 2.5 and 2.7 ppm, corresponding to the epoxide group of the PBO segment in the PS-*b*-PBO copolymer. Figure 1 also assigns all of the other signals to the hydrogen atoms of the PS-*b*-PB and PS-*b*-PBO block copolymers. The FT-IR spectroscopic analysis shown in Figure 2 confirms the epoxidation of the characteristic signals of the C=C bond. The characteristic

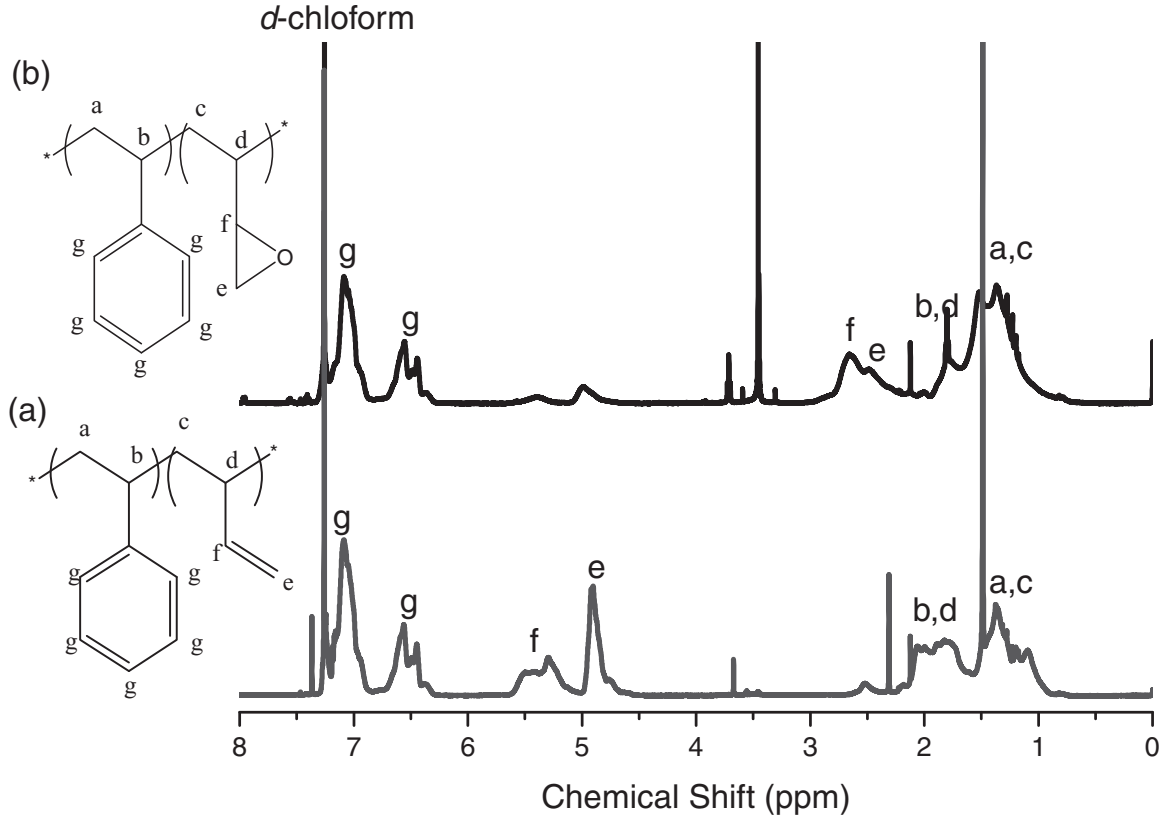

Figure 1. ^{1}H NMR spectra of a) PS-*b*-PB and b) PS-*b*-PBO diblock copolymers in $CDCl_3$.

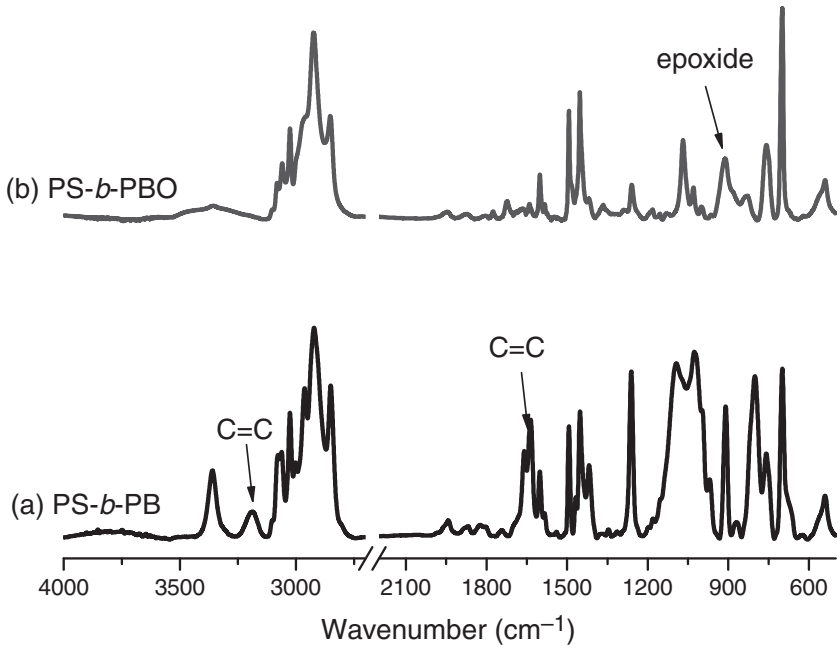

Figure 2. FT-IR spectra of a) PS-*b*-PB and b) PS-*b*-PBO diblock copolymers at room temperature.

absorption bands of the allyl group of the PB segment that appear at 3186 (stretching of =C–H bonds), 1636, and 1658 cm^{-1} (stretching of C=C bonds)[46] disappeared after epoxidation. A new band for the epoxide ring of the PBO segment appeared at 914 cm^{-1}.[47] Figure 3 shows typical second-run DSC thermograms of the PS-*b*-PB and PS-*b*-PBO copolymers. The PS-*b*-PBO copolymer (T_g = −7 and 110 °C) clearly exhibits two glass transitions, indicating that the chemical incompatibility between the constituent blocks leads to microphase separation. The lower T_g corresponds to the PB block, and the higher T_g corresponds to the PS block segments. In addition, the T_g of the PS block in the diblock copolymers was higher than that in the PS homopolymer, presumably because of the high molecular weight of the PS ($\overline{M}_n$ = 200 000 g mol^{-1}) used in this study. Clearly, the change of the T_g value (−7 °C) of the PB block

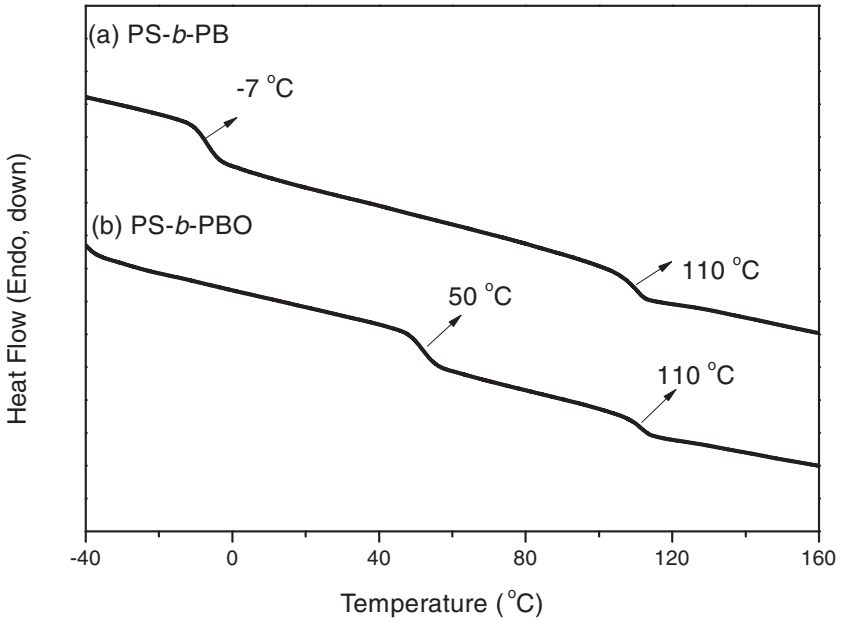

Figure 3. DSC thermograms of a) PS-*b*-PB and b) PS-*b*-PBO diblock copolymers.

to 50 °C with respect to the PBO block in the PS-*b*-PBO copolymer is attributable to the fact that the higher polarity of PBO than that of the PB segments decreased the free volume of the chain segments. The ^{1}H NMR, FT-IR, and DSC results indicate the successful synthesis of the PS-*b*-PBO copolymer.

3.2. The Crosslinking Reaction of the PS-*b*-PBO Copolymer with Poly(ethylene oxide bisamine)

Stoichiometric amounts of poly(ethylene oxide bisamine) (D230) an PS-*b*-PBO diblock copolymer were mixed in a high-speed stirrer in toluene. The toluene solution contained 20 wt% of the PS-*b*-PBO diblock copolymers. The solution as cast into films and dried under vacuum. Figure 4 shows the infrared spectra of PS-*b*-PBO with D230 at various temperatures, where the molar ratio of the epoxide group of PBO is equal to that of the bisamine group of D230 (100 mol% of D230). The epoxide peak at 914 cm^{-1} for PBO disappeared, and a broad band absorption at ca. 3477 cm^{-1} of the secondary hydroxy group, formed by the

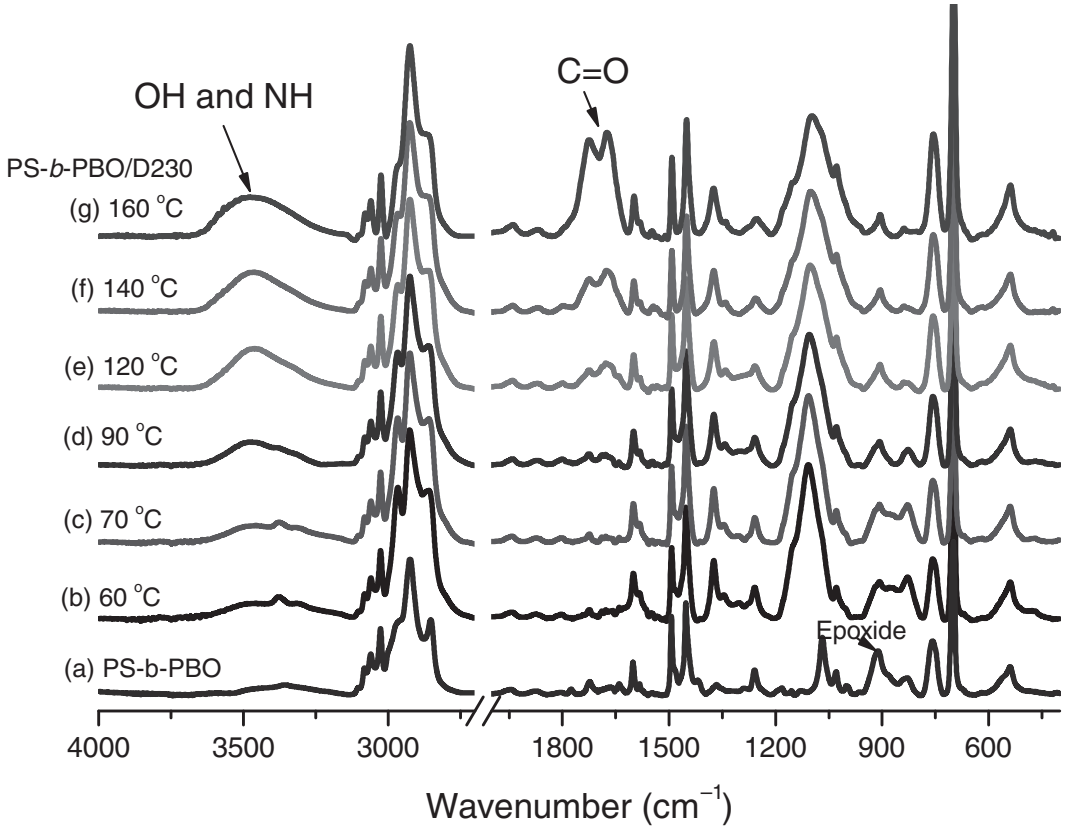

Figure 4. FT-IR spectra of PS-*b*-PBO/D230 thermal curing with various temperatures.

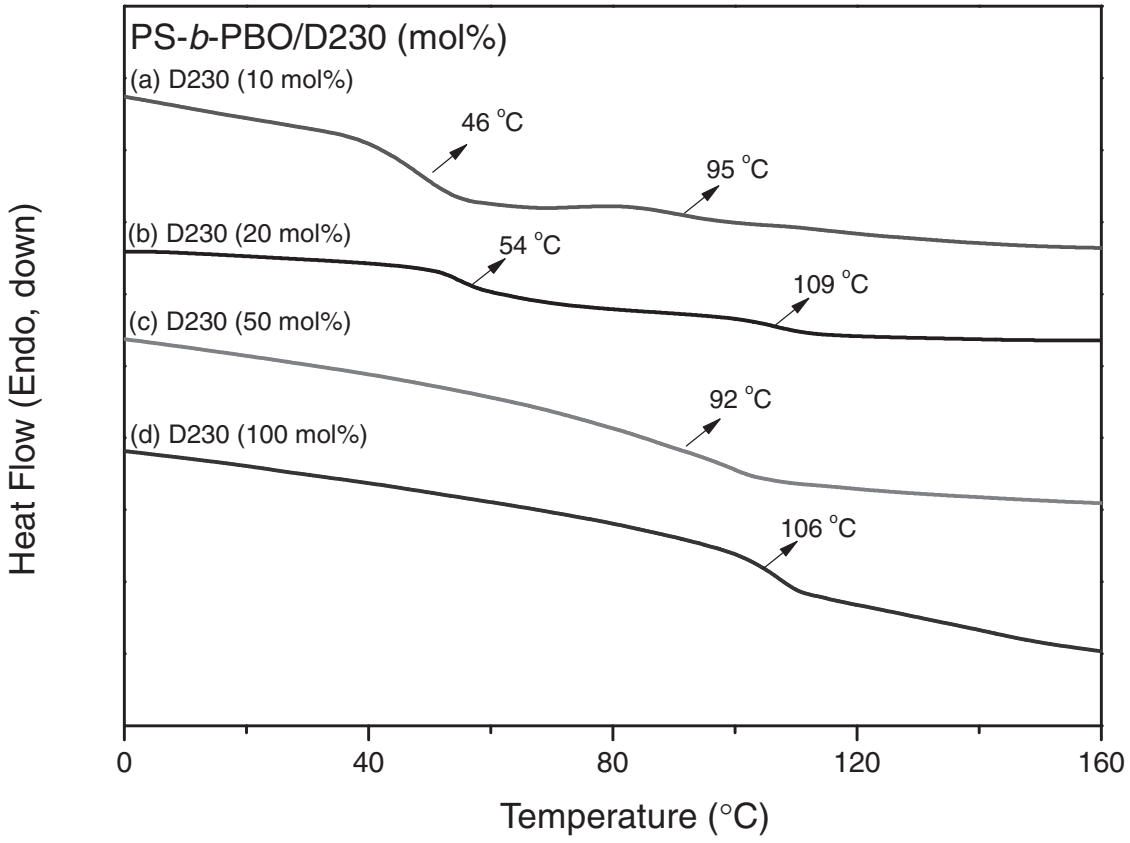

Figure 5. DSC thermograms of PS-*b*-PBO diblock copolymers with different amounts of D230 content after thermal curing.

ring-opening reaction of the epoxy group, and amine group from the curing agent D230, increased with temperature, indicating that the crosslinking reaction had occurred under a thermal reaction without a catalyst. The curing reaction is also summarized in Scheme 1. In addition, new absorptions at 1730 and 1674 cm^{-1} were observed at relatively higher temperatures, corresponding to the formation of carbonyl (C=O) and amide (CONH) groups from the oxidation of the hydroxy and amine groups after the crosslinking reaction. As a result, the crosslinking reaction between PS-*b*-PBO and D230 should be performed at 70 °C according to Figure 4 to avoid the oxidation reaction that occurred in this study. Figure 5 shows typical second-run DSC thermograms of PS-*b*-PBO with different amounts of D230 after thermal crosslinking; two distinct T_g values can be observed at relatively lower D230 contents (10 and 20 mol%), which correspond to the PS phase and the crosslinking mixed phase of PBO/D230, respectively. The T_g of the PBO/D230 mixed phase shifted toward higher values with increasing D230 contents and produced only one T_g, suggesting that these PS-*b*-PBO/D230 blends possess a disordered structure at relatively higher D230 contents (50 and 100 mol%).

3.3. The Synthesis of 2-Phenylethanethiol Au NPs

The 2-phenylethanethiol Au NPs used in this study were prepared through the standard Brust–Schiffrin methodology. The chemical structure of 2-phenylethanethiol Au NPs is shown in Figure 6a. The TEM image of phenylethanethiol-functionalized Au NPs shown in Figure 6b reveals that the diameter of the Au core is 2.5 ± 0.3 nm. Figure 6c shows the UV-vis spectra of the 2-phenylethanethiol Au NPs in toluene (300–800 nm). The maxima absorption in toluene is at 521 nm for Au NPs. In the framework of the Mie theory,[48] the position of the maximum of the absorption band is determined by the refractive index of the medium surrounding the NPs, while the width is controlled by the particle size. The observed invariant width reveals the absence of particle aggregation and that the particle edge–edge distances are the same. The same absorption maximum at 521 nm suggests the same dipole–dipole interaction, implying that the desorption of the Au–S thiolate covalent bond does not occur. The atomic composition of the Au NPs was determined by using thermogravimetric analysis (TGA),[41] which showed that 71.2% of the sample was gold by mass, as shown in Figure 6d. The first step in the TGA was

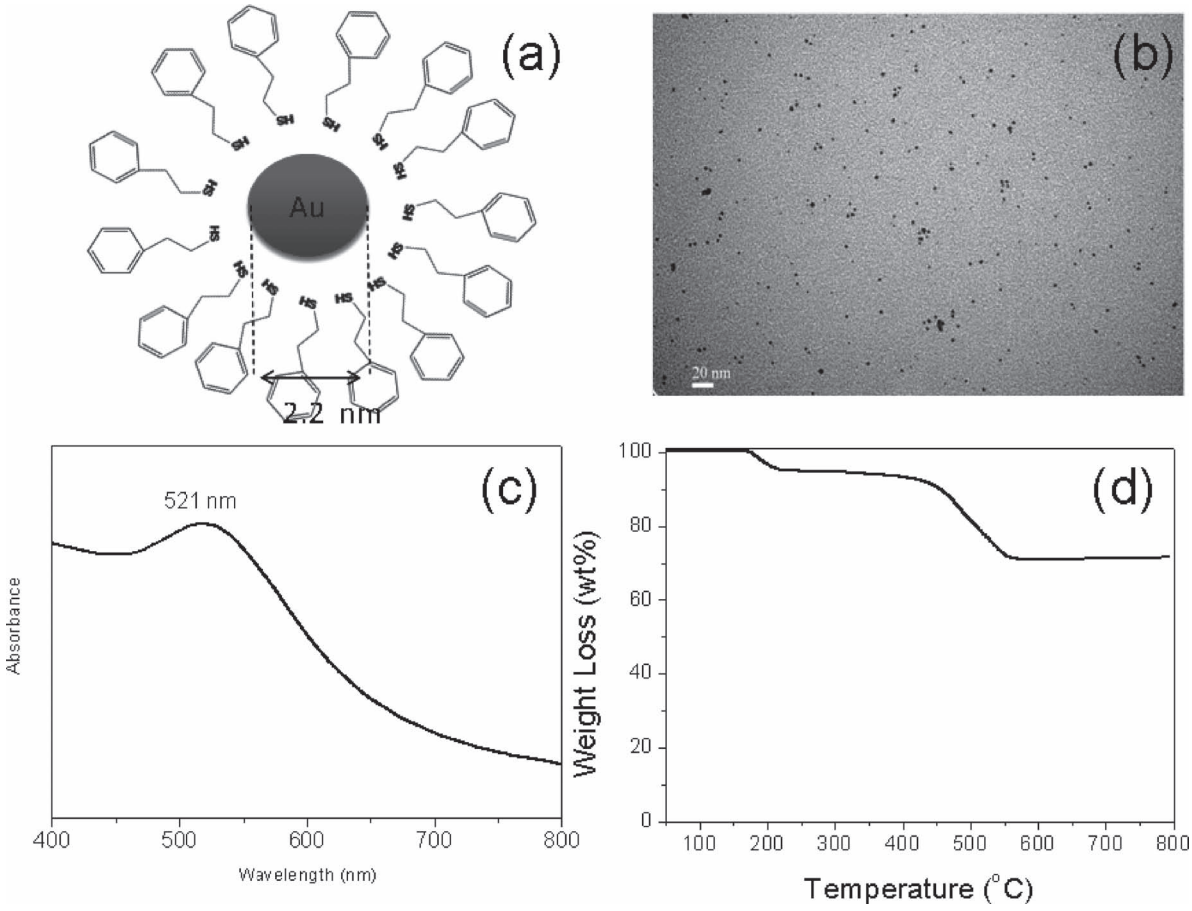

Figure 6. a) Chemical structure, b) TEM image, c) UV-vis spectra, and d) TGA analysis of 2-phenylethanethoil Au NPs.

attributable to the decomposition of the ethane group, and the second step was a result of decomposition of the benzene group from 2-phenylethanethiol.

3.4. The Preparation of Au NP/PS-*b*-PBO Diblock Copolymer Composites

SAXS analyses were preformed to quantify the *d*-spacing of polymer chains after the Au NPs were incorporated.[44] Figure 7 shows the SAXS patterns of a PS-*b*-PBO block copolymer containing different amounts of 2-phenylethanethiol Au NPs. The intensity in the low-*q* region (between 0.03 and 0.08 $Å^{-1}$) remained almost constant with the increase in the Au NP content. The primary peak corresponding to microphase separation and the self-assembled structure of the PS-*b*-PBO block was not observed because the Au NPs produce a much higher

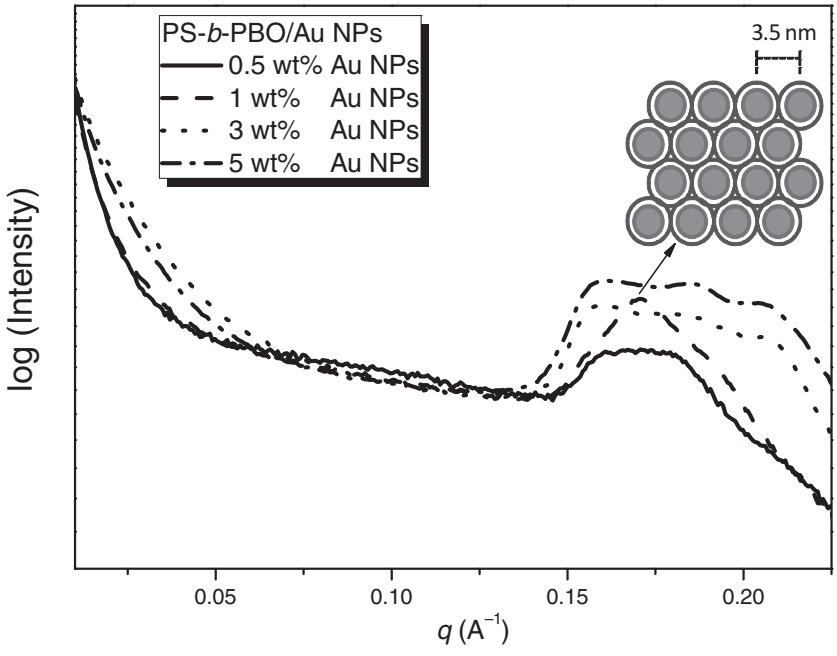

Figure 7. SAXS patterns of the PS-*b*-PBO block copolymer containing different amounts of 2-phenylethanethiol Au NPs.

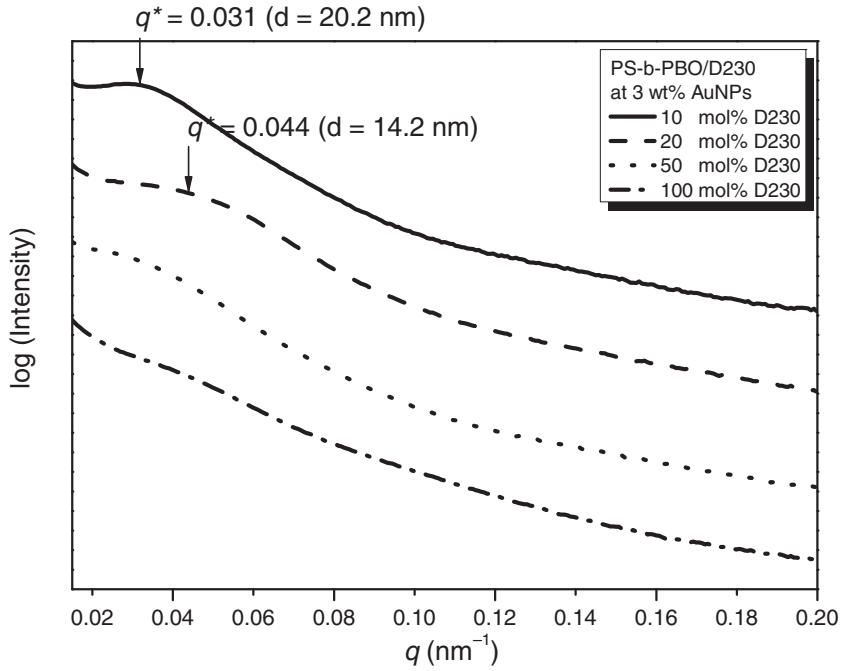

Figure 8. SAXS patterns of the Au NP/PS-*b*-PBO/D230 composites containing different D230 contents at 3 wt% of Au NPs.

intensity than random dispersions or aggregates of Au NPs by coherent or constructive interference.[44] In addition, the strong scattering peak of the composite at a q value of ca. 0.18 Å^{-1} suggests a liquid-like ordering of Au NPs. The mean spacing of this peak is ca. 3.5 nm, which corresponds well with the diameter of the Au NPs (2.2 nm) plus twice the length of the 2-phenylethanethiol ligand (2 × 0.7 nm = 1.4 nm),[44] as is shown in Figure 7.

Figure 8 shows SAXS patterns of the Au NP/PS-*b*-PBO/D230 composites containing different amounts of D230 but fixed at 3 wt% of Au NPs. Clearly, the peak of the Au NPs clusters at ca. 0.18 Å^{-1} completely disappeared after crosslinking with D230, indicating a structural transformation by the incorporation of Au NPs in this case. In addition, it shows the first-order scattering broad peak that corresponds to a Bragg spacing of 20.2 nm, the average spacing between the PS and neighboring PBO/D230 microphase at 10 mol% of D230. The average spacing between the neighboring microdomains decreased to 14.2 nm at 20 mol% of D230 because of the higher degree of crosslinking than that with 10 mol% of D230, which would be expected to shrink the d-spacing of the block copolymer. At increasingly higher D230 contents, the primary first peak disappeared, which is consistent with the DSC analyses (only one T_g at higher D230 contents). Combining the DSC and SAXS results, we can conclude that the Au NP/PS-*b*-PBO/D230 system features short-range-order nanostructures at lower D230 content (20 mol%) and that Au NPs diffuse to the interfaces between PS and PBO.

Figure 9a shows TEM images of Au NP/PS-*b*-PBO without the D230 curing agent at 3 wt% of Au NPs. The TEM specimen was prepared by dipping a carbon-coated copper grid and drying under vacuum. The TEM image indicates that the Au NPs aggregate together after the evaporation of toluene, and no individual NPs are observed outside of the structure; most

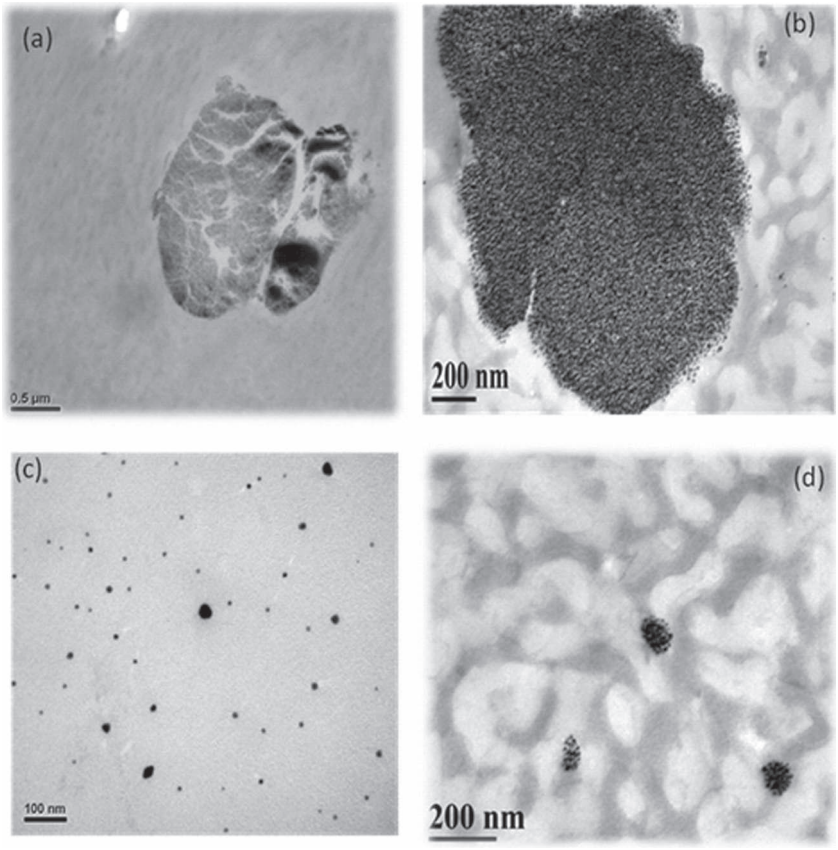

Figure 9. TEM images of PS-*b*-PBO/Au NP composites at 3 wt% Au NPs a) without D230 curing agent and then stained withRuO_4 (b), and c) with 10 mol% D230 curing agent, and then stained with RuO_4 (d).

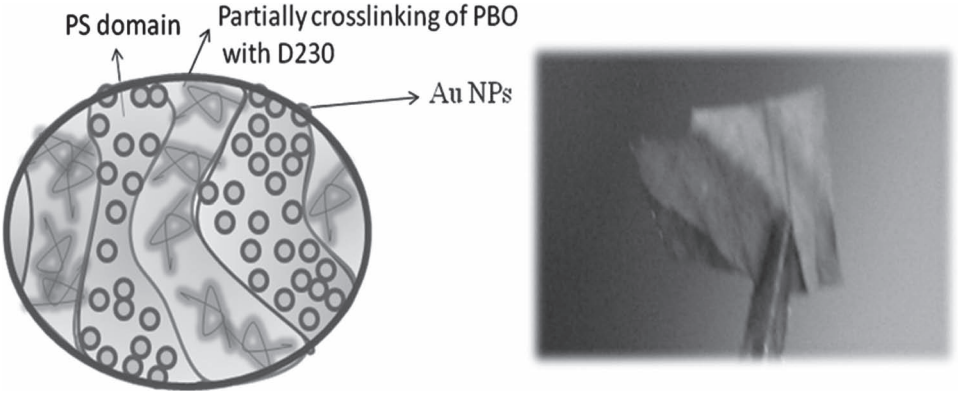

Scheme 2. The possible morphology of Au NP/PS-*b*-PBO/D230 composites and a corresponding image of the Au NP/block copolymer composite.

of these Au NPs form aggregates more than several hundred nanometers in dimension. After 30 min of staining with RuO_4 at room temperature, the gray PS phase and Au NPs that aggregated could be observed as shown in Figure 9b, indicating that the 2-phenylethanethiol Au NPs accumulate in both blocks. This means that the π–π interactions between the phenyl groups of the Au NPs and PS segments are significantly weaker than the aggregation ability of the Au NPs that diffuse to the interfaces between the PS and PBO blocks. To limit the grain growth of the Au NP aggregates in the PBO domains, the partial crosslinking of PBO was used in this study. Figure 9c shows TEM images of Au NP/PS-*b*-PBO composites with the D230 (10 mol%) curing agent at 3 wt% of Au NPs. Randomly distributed Au NPs can be observed in the TEM image, which means that the 2-phenylethanethiol-stabilized Au NPs do not aggregate and that the partial crosslinking of PBO prohibits the diffusion of Au NPs to the PBO domains. The 2-phenylethanethiol Au NPs were located only in the PS/PBO interface dominantly, as confirmed by Figure 9d after staining with RuO_4 for 30 min; the possible morphology of the Au NP/PS-*b*-PBO/D230 composite is shown in Scheme 2.

Figure 10 shows the UV-vis spectra of Au NP/PS-*b*-PBO composites at various Au NP contents without the D230 curing agent. The absence of a plasmon absorption band indicates the strong aggregation of Au NPs in all cases, which is consistent with TEM and SAXS analyses. Figure 11 shows the UV-vis spectra of Au NP/PS-*b*-PBO composites with different amounts of D230 curing agent at 3 wt% Au NPs. The maxima absorption in toluene is at 521 nm for pure Au NPs. A red shift of the plasmon absorption was clearly observed with the increase in the D230 curing agent content. Previous studies have proven that the aggregation of Au NPs leads to a red shift of the plasmon absorption because of the electronic coupling interaction between neighboring particles.[38] The maximum absorbance of the Au NPs shifted to 533 nm (10 mol% D230) and 550 nm (20 mol% D230) because of the segregation of NPs at the PS and PBO interface. Moreover, when Au NPs are brought into close contact with one another, plasmon resonance coupling of the colloids results in a red shift of the plasmon band; this is consistent with the results of the SAXS analysis, which show that the average spacing between

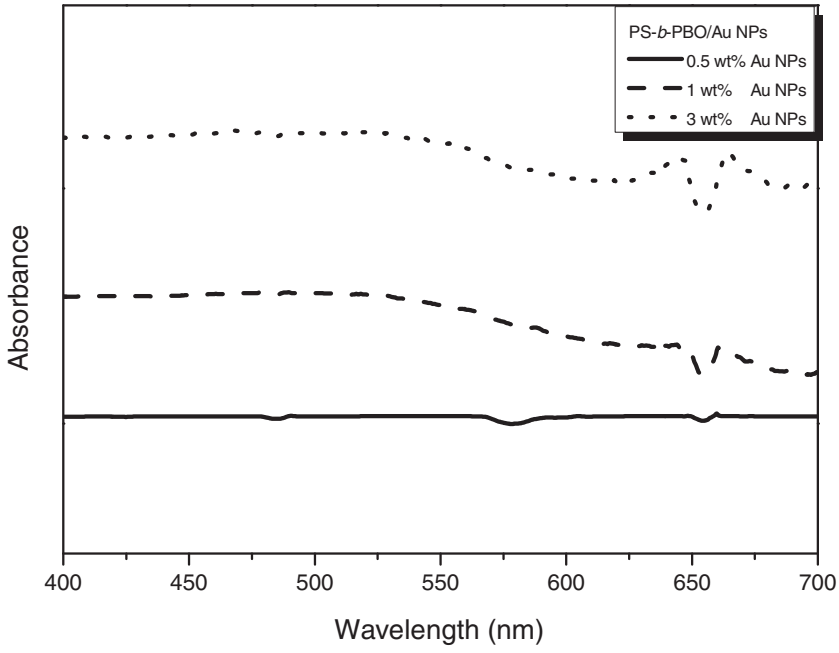

Figure 10. UV-vis spectra of Au NP/PS-*b*-PBO composites at various Au NP contents without D230 curing agent.

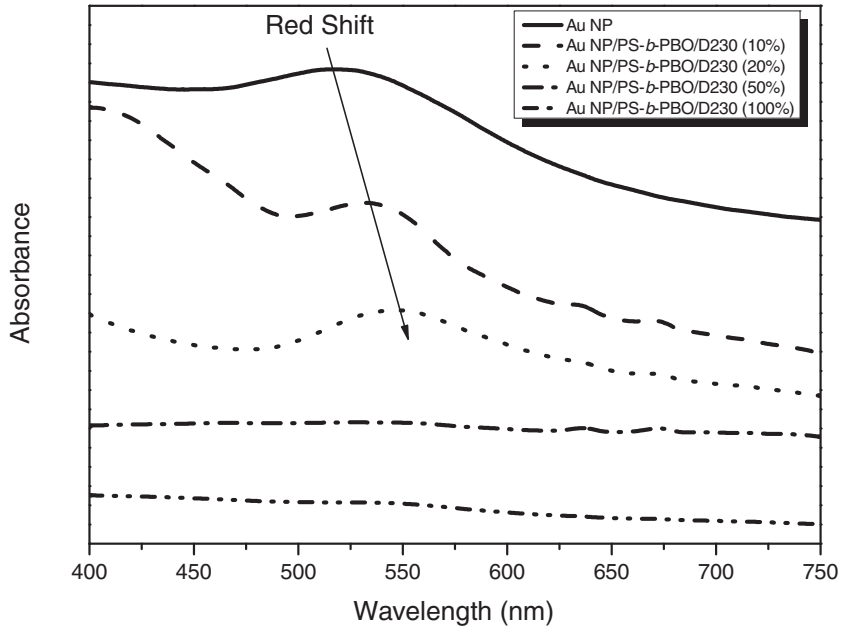

Figure 11. UV-vis spectra of Au NP/PS-*b*-PBO composites with different amounts of D230 curing agent at 3 wt% Au NPs.

the neighboring microdomains decreases from 20.2 (10 mol% D230) to 14.2 nm (20 mol% D230). The probability of Au NPs closely contacting one another becomes higher and results in a red shift of the plasmon band. However, this maximum absorbance disappears at relatively higher D230 contents (>50 mol%), indicating the strong aggregation of Au NPs located in both the PS and PBO phase. This result is consistent with SAXS and DSC analyses, through which microphase separation was not observed at higher D230 contents (>50 mol%).

4. Conclusion

We have synthesized a new epoxidated PS-*b*-PBO diblock copolymer through chemical modification of PS-*b*-PB with *meta*-chloroperoxybenzoic acid. A new uniform size distribution of the metal core of Au NPs could be finely tuned by using 2-phenylethanthiol as stabilizer. Au NPs could disperse in the PS-*b*-PBO at the molecular level, the absence of aggregates in the PS domains was achieved, and the partial crosslinking of PBO with a D230 curing agent prohibited the Au NPs from diffusing to the PBO block segment. The materials that can be fabricated by this method can potentially exhibit enhanced electric, optical, magnetic, or catalytic properties because of the inorganic NPs incorporated into the block copolymer structure.

Acknowledgements: This study was supported financially by the National Science Council, Taiwan, Republic of China, under contracts NSC 97-2221-E-110-013-MY3 and NSC 99-2628-E-110-003.

Received: June 23, 2011; Published online: September 7, 2011; DOI: 10.1002/macp.201100360

Keywords: block copolymers; gold nanoparticles; self-assembly

[1] M. A. El-Sayed, *Acc. Chem. Res.* **2001**, *34*, 257.
[2] C. P. Collier, T. Vossmeyer, J. R. Heath, *Annu. Phys. Chem.* **1998**, *49*, 371.
[3] Z. Konya, V. F. Puntes, I Kiricsi, J. Zhu, J. W. Ager, M. K. Ko, H. Frei, P. Alivisatos, G. A. Somorjai, *Chem. Mater.* **2003**, *15*, 1242.
[4] C. H. Lu, S. W. Kuo, C. F. Huang, F. C. Chang, *J. Phys. Chem. C* **2009**, *113*, 3517.
[5] S. W. Kuo, Y. C. Wu, C. H. Lu, F. C. Chang, *J. Polym. Sci., Part B: Polym. Phys.* **2009**, *47*, 811.
[6] S. D. Lin, M. Bollinger, M. A. Vannice, *Catal. Lett.* **1993**, *17*, 245.
[7] M. Okumura, T. Akita, M. Haruta, *Catal. Today* **2002**, *74*, 265.
[8] C. Milone, M. L. Tropeano, G. Gulino, G. Neri, R. Ingoglia, S. Galvagno, *Chem. Commun.* **2002**, 868.
[9] K. Blick, T. D. Mitrelias, J. S. J. Hargreaves, G. J. Hutechings, R. W. Joyner, C. J. Kiely, F. E. Wagner, *Catal. Lett.* **1998**, *50*, 211.
[10] R. J. H. Grisel, P. J. Kooyman, B. E. Nieuwenhuys, *J. Catal.* **2000**, *191*, 430.
[11] T. M. Salama, R. Ohnishi, T. Shido, M. Ichikawa, *J. Catal.* **1996**, *162*, 169.
[12] M. R. Bockstaller, R. A. Mickiewicz, E. L. Thomas, *Adv. Mater.* **2005**, *17*, 1331.
[13] M. Lazzari, M. A. Lopez-Quintela, *Adv. Mater.* **2003**, *15*, 1583.
[14] C. Burda, X. B. Chen, R. Narayanan, M. A. El-Sayed, *Chem. Rev.* **2005**, *105*, 1025.
[15] L. Zhu, S. Z. D. Cheng, P. Huagn, Q. Ge, R. P. Quirk, E. L. Thomas, B. Lozt, B. S. Hsiao, F. Yeh, L. Liu, *Adv. Mater.* **2002**, *14*, 31.
[16] J. Z. Zhang, *Acc. Chem. Res.* **1997**, *30*, 423.
[17] P. Simon, U. Schwarz, R. Kniep, *J. Mater. Chem.* **2005**, *15*, 4992.
[18] M. J. Birnkrant, C. Y. Li, V. Natarajan, V. P. Tondiglia, R. L. Sutherland, R. F. Lloyd, T. J. Bunning, *Nano Lett.* **2007**, *7*, 3128.
[19] F. Cheng, K. Zhang, D. Chen, L. Zhu, M. Jiang, *Macromolecules* **2009**, *42*, 7108.
[20] R. Vaia, J. Baur, *Science* **2008**, *319*, 420.
[21] R. R. Bockstaller, Y. Lapetnikov, S. Margel, E. L. Thomas, *J. Am. Chem. Soc.* **2003**, *125*, 5276.
[22] J. Y. Lee, R. B. Thompson, D. Jasnow, A. C. Balazs, *Macromolecules* **2002**, *35*, 4855.
[23] A. C. Balazs, T. Emrick, T. P. Russell, *Science* **2006**, *314*, 1107.
[24] J. Y. Cheng, C. A. Ross, H. I. Smith, E. L. Thomas, *Adv. Mater.* **2006**, *18*, 2505.
[25] J. Listak, I. F. Hakem, H. J. Ryu, S. Rangou, N. Politakos, K. Misichronis, A. Avgeropoulos, M. R. Bockstaller, *Macromolecules* **2009**, *42*, 5766.

[26] A. J. Schultz, C. K. Hall, J. Genzer, *Macromolecules* **2005**, *38*, 3007.
[27] J. Kim, P. F. Green, *Macromolecules* **2010**, *43*, 10452.
[28] D. Ray, V. K. Aswal, J. Kohlbrecher, *Langmuir* **2011**, *27*, 4048.
[29] S. G. Lopez, E. Castro, P. Taboada, V. Mosquera, *Langmuir* **2008**, *24*, 13186.
[30] T. Azzam, A. Eisenberg, *Langmuir* **2007**, *23*, 2126.
[31] S. G. Lopez, P. Taboada, A. Cambon, J. Juarez, A. Alvarez-Lorenzo, A. Coucheiro, V. Mosquera, *J. Phys. Chem. B* **2010**, *114*, 66.
[32] K. Rahme, F. Gauffre, J. D. Marty, B. Payre, C. Mingotaud, *J. Phys. Chem. C* **2007**, *111*, 7273.
[33] B. J. Kim, J. Bang, C. J. Hawker, J. J. Chiu, D. J. Pine, S. G. Jang, S. M. Yang, E. J. Kramer, *Langmuir* **2007**, *23*, 12693.
[34] S. N. Sidorov, L. M. Bronstein, Y. A. Kabachii, P. M. Valetsky, P. L. Soo, D. Maysinger, A. Eisenberg, *Langmuir* **2004**, *20*, 3543.
[35] G. Hou, L. Zhu, D. Chen, M. Jiang, *Macromolecules* **2007**, *40*, 2134.
[36] W. J. Shin, F. Basarir, T. H. Yoon, J. S. Lee, *Langmuir* **2009**, *25*, 3344.
[37] B. J. Kim, G. H. Fredrickson, C. J. Hawker, E. J. Kramer, *Langmuir* **2007**, *23*, 7804.
[38] C. C. Chang, C. T. Lo, *J. Phys. Chem. B* **2011**, *115*, 2485.
[39] R. M. Ho, T. Lin, M. R. Jhong, T. M. Chung, B. T. Ko, Y. C. Chen, *Macromolecules* **2005**, *38*, 8607.
[40] C. H. Lu, C. F. Huang, S. W. Kuo, F. C. Chang, *Macromolecules* **2009**, *42*, 1067.
[41] M. K. Corbierre, N. S. Cameron, M. Sutton, S. G. J. Mochrie, L. B. Lurio, A. Ruhm, R. B. Lennox, *J. Am. Chem. Soc.* **2001**, *123*, 10411.
[42] H. Yockell-Lelievre, D. Gingras, R. Vallee, A. M. Ritcey, *J. Phys. Chem. C* **2009**, *113*, 21293.
[43] J. Tian, J. Jin, F. Zheng, H. Zhao, *Langmuir* **2010**, *26*, 8762.
[44] C. M. Huang, K. H. Wei, U. S. Jeng, K. S. Liang, *Macromolecules* **2007**, *40*, 5067.
[45] T. Yonezawa, K. Yasui, N. Kimizuka, *Langmuir* **2001**, *17*, 271.
[46] K. W. Huang, S. W. Kuo, *Macromol. Chem. Phys.* **2010**, *211*, 2301.
[47] S. W. Kuo, W. C. Liu, *J. Appl. Polym. Sci.* **2010**, *117*, 3121.
[48] H. Hovel, S. Fritz, A. Hilger, U. Kreibig, M. Vollmer, *Phys. Rev. B* **1993**, *48*, 178.